

*Citation for published version:*

Ramin, P, Brock, AL, Causanilles, A, Valverde-Pérez, B, Emke, E, de Voogt, P, Polesel, F & Plosz, BG 2017, 'Transformation and sorption of illicit drug biomarkers in sewer biofilm', *Environmental Science and Technology*, vol. 51, no. 18, pp. 10572-10584. <https://doi.org/10.1021/acs.est.6b06277>

*DOI:*

[10.1021/acs.est.6b06277](https://doi.org/10.1021/acs.est.6b06277)

*Publication date:*

2017

*Document Version*

Peer reviewed version

[Link to publication](https://doi.org/10.1021/acs.est.6b06277)

This document is the Accepted Manuscript version of a Published Work that appeared in final form in *Environmental Science and Technology*, copyright © American Chemical Society after peer review and technical editing by the publisher. To access the final edited and published work see <https://doi.org/10.1021/acs.est.6b06277>.

**University of Bath**

## **Alternative formats**

If you require this document in an alternative format, please contact:  
[openaccess@bath.ac.uk](mailto:openaccess@bath.ac.uk)

### **General rights**

Copyright and moral rights for the publications made accessible in the public portal are retained by the authors and/or other copyright owners and it is a condition of accessing publications that users recognise and abide by the legal requirements associated with these rights.

### **Take down policy**

If you believe that this document breaches copyright please contact us providing details, and we will remove access to the work immediately and investigate your claim.

# Transformation and sorption of illicit drug biomarkers in sewer biofilms

Pedram Ramin<sup>a,b,\*</sup>, Andreas Libonati Brock<sup>a</sup>, Ana Causanilles<sup>c</sup>, Borja Valverde-Pérez<sup>a</sup>, Erik Emke<sup>c</sup>, Pim de Voogt<sup>c,d</sup>, Fabio Polesel<sup>a</sup>, Benedek Gy. Plósz<sup>a,e,\*</sup>

<sup>a</sup>Department of Environmental Engineering, Technical University of Denmark (DTU), Bygningstorvet, Bygning 115, 2800 Kgs. Lyngby, Denmark

<sup>b</sup>Process and Systems Engineering Center (PROSYS), Department of Chemical and Biochemical Engineering, Technical University of Denmark, Building 229, 2800 Kgs. Lyngby, Denmark

<sup>c</sup>KWR Watercycle Research Institute, P.O. Box 1072, 3430 BB Nieuwegein, The Netherlands`1

<sup>d</sup>Institute for Biodiversity and Ecosystem Dynamics, University of Amsterdam, P.O. Box 94248, 1090 GE Amsterdam, The Netherlands

<sup>e</sup>Department of Chemical Engineering, University of Bath, Claverton Down, Bath BA2 7AY,UK

\*Corresponding authors: [pear@kt.dtu.dk](mailto:pear@kt.dtu.dk); [b.g.plosz@bath.ac.uk](mailto:b.g.plosz@bath.ac.uk)

---

## Abstract

In-sewer transformation of drug biomarkers (excreted parent drugs and metabolites) can be influenced by the presence of biomass in suspended form as well as attached to sewer walls (biofilms). Biofilms are likely the most abundant and biologically active biomass fraction in sewers. In this study, 16 drug biomarkers were selected, including the major human metabolites of mephedrone, methadone, cocaine, heroin, codeine and tetrahydrocannabinol (THC). Transformation and sorption of these substances were assessed in targeted batch experiments using laboratory-scale biofilm reactors operated under aerobic and anaerobic conditions. A one-dimensional model was developed to simulate diffusive transport, abiotic and biotic transformation and partitioning

of drug biomarkers. Model calibration to experimental results allowed estimating transformation rate constants in sewer biofilms, which were compared to those obtained using in-sewer suspended biomass.

Our results suggest that sewer biofilms can enhance the transformation of most compounds. Through scenario simulations, we demonstrated that the estimation of transformation rate constants in biofilm can be significantly biased if the boundary layer thickness is not accurately estimated. This study complements our previous investigation on the transformation and sorption of drug biomarkers in the presence of only suspended biomass in untreated sewage. A better understanding of the role of sewer biofilms—also relative to the in-sewer suspended solids—and improved prediction of associated fate processes can lead to more accurate estimation of daily drug consumption in urban areas in wastewater-based epidemiological assessments.

## Introduction

Wastewater-based epidemiology (WBE) has emerged as a new paradigm to monitor trends of community-wide drug use based on chemical analysis of urinary drug biomarkers in raw sewage, typically in the influent of wastewater treatment plants (WWTPs).<sup>1,2</sup> Transport in upstream sewer pipelines is known to influence the quality of untreated wastewater<sup>3</sup>, hence reliable estimations of drug use based on observations in WWTP influents require consideration of in-sewer transformations and sorption of biomarkers. A recent investigation<sup>4</sup> in a full-scale pressurized sewer pipeline revealed significant elimination or formation of pharmaceuticals (e.g. bezafibrate and sulfamethoxazole, respectively).

The uncertainty introduced by neglecting in-sewer processes is often ignored<sup>5</sup> among other sources of uncertainty in WBE studies.<sup>6</sup> The *in-sample* stability of drug biomarkers has been widely assessed<sup>7–10</sup>, providing an indication of biotransformation in raw wastewater. These studies prominently addressed the reliability of analysis after sample collection, focusing e.g. on biomarker stability during composite sample collections, rather than refining back-calculation schemes by accounting for in-sewer transformations. However, due to differences in operation and design of sewer systems, *in-sewer* stability of drugs of abuse is not only compound-specific but also highly dependent upon the catchment layout (e.g., size<sup>11</sup>) and the hydraulic conditions in the pipelines.

Moreover, in-sewer fate processes are not limited to biotransformation in the bulk phase and biofilms/sediments, but also include abiotic processes and partitioning of drug biomarkers to suspended and attached solids. Drug biomarkers can be in-sewer transformation product of other human metabolites and hence their concentration can be significantly influenced. When considering these challenges, chemical *stability* in terms of percentage removal efficiency or correction factors (lumped factors that include excretion ratio, in-sewer transformation etc.) cannot be a reliable source of information for the estimation of drug load at the point of excretion.

Recently, transformation and sorption of several drug biomarkers in raw wastewater in the presence of suspended biomass have been assessed using targeted experiments and mechanistic modelling.<sup>12</sup> This previous study elucidated the role of only one of the possible actors of in-sewer biochemical processes, as biomass in sewer systems is present also in attached form. However, limited evidence exists on the role of sewer biofilms. To date, only a few studies<sup>13,14</sup> assessed removal kinetics in sewer biofilms, showing enhanced relative removal efficiency of selected drug biomarkers (cocaine and 6-mono-acetylmorphine) as compared to raw wastewater. Nevertheless, a number of previously uninvestigated factors are likely to influence (the estimation of) biofilm-mediated transformation rates, namely (i) sorption onto biofilm<sup>15</sup>, similarly to suspended solids in untreated wastewater<sup>12</sup>; (ii) concurrent transformation and formation from other biomarkers<sup>8,12,16,17</sup>; (iii) abiotic degradation<sup>5,12</sup>; (iv) prevailing redox conditions (aerobic and anaerobic); and (v) diffusive transport through boundary layer and in biofilm<sup>15,18</sup>. While being typically neglected in biotransformation studies with biofilms, The impact of (v) may be substantial considering the structure and the thickness of sewer biofilms and the reduced diffusivity of large organic molecules.<sup>19–21</sup> This is especially important in pressurized sewers, where sewer biofilms are abundant in completely filled pipes.<sup>3,22</sup>

In this study, we sought to improve the existing understanding of the fate of drug biomarkers in the presence of sewer biofilms by means of an experimental and model-based assessment. This study was meant to complement our previous investigation<sup>12</sup> on the fate of drug biomarkers in untreated sewage, in the presence of only suspended biomass. The objectives of our investigation were thus: (i) to assess the transformation and sorption of 16 drug biomarkers in sewer biofilms under aerobic and anaerobic conditions (using laboratory-scale rotating biofilm reactors); (ii) to model the fate of selected drug biomarkers in the biofilm by explicitly describing diffusive transport and reaction kinetics;

(iii) to estimate biofilm-mediated biotransformation kinetics for the selected biomarkers, and to compare them with transformation kinetics by suspended biomass in untreated wastewater.

## Materials and methods

**Selection of trace organic biomarkers.** Six illicit drugs were selected based on their high consumption levels according to a recent European report.<sup>23</sup> The target list was completed with 10 human metabolites and included: (i) mephedrone (MEPH); (ii) methadone (METD) and its metabolite 2-ethylidene-1,5-dimethyl-3,3-diphenylpyrrolidine (EDDP); (iii) cocaine (COC) and its metabolites benzoylecgonine (BE), ecgonine methyl ester (EME), and cocaethylene (CE); (iv) heroin (HER) and its metabolites 6-monoacetylmorphine (6-MAM), morphine (MOR), and morphine-3- $\beta$ -D-glucuronide (MORG); codeine (COE) and its metabolite norcodeine (NCOE); (v) tetrahydrocannabinol (THC) and its metabolites 11-hydroxy- $\Delta^9$ -THC (THCOH), and 11-nor-9-carboxy- $\Delta^9$ -THC (THCCOOH). COE and NCOE were also considered in the same group as MOR, since COE can potentially transform to MOR and NCOE during human metabolism.<sup>24</sup> Analytical Standards (IS) and isotopically labeled internal standard (ILIS) analogues from Sigma Aldrich (Brøndby, Denmark) were dissolved in methanol or acetonitrile at concentrations of 0.1 mg mL<sup>-1</sup> and 1 mg mL<sup>-1</sup>, respectively. Poor data quality prevented us from assessing the transformation of methamphetamine and amphetamine, which are widely used in Europe.<sup>23</sup>

**Experimental set-up with continuous-flow operation.** Two annular rotating biofilm reactors, made of poly(methyl methacrylate) (Plexiglas), operated either under aerobic or anaerobic conditions with operating volume of 0.961 L, were used to simulate in-sewer conditions by controlling, e.g., shear conditions on biofilm. The reactors consisted of an inner rotating drum (diameter=9.0 cm) and an outer stationary cylinder (diameter=11.4 cm), supporting the growth of attached biomass. This type of reactor provided for high surface area to volume ratio (175 m<sup>2</sup> m<sup>-3</sup>) that could be advantageous for biofilm growth. Each reactor was equipped with four removable slides, allowing for inspection of biofilm during reactor operation.

In order to establish stable aerobic and anaerobic biofilms, the two reactors were operated under continuous-flow conditions for more than 7 months while being kept in the dark. The rotation speed of the reactors was set to 20 rpm. The wall shear stress was calculated according to equations provided by Rochex et al.<sup>25</sup> as

0.05 Pa which is in the lower range of typical wall shear stress in the sewers, measured up to 3 Pa in a gravity sewer.<sup>26</sup> Low shear stress was chosen in order to decrease biofilm sloughing and therefore enhance biofilm thickness. The reactors were continuously fed ( $4 \text{ L d}^{-1}$ , hydraulic residence time of approximately  $0.25 \text{ d}^{-1}$ ) with pre-clarified wastewater from external cooled containers ( $T \leq 4^\circ\text{C}$ ) that were sparged with dry compressed atmospheric air (aerobic reactor) or nitrogen (anaerobic reactor). The experiments were performed to mimic completely aerobic and anaerobic redox conditions. The external tanks were filled with pre-clarified wastewater collected from Mølleåværket WWTP (Lundtofte, Denmark) semi-weekly. The wastewater had following characteristics: soluble organic carbon, expressed as chemical oxygen demand (COD) =  $40\text{--}130 \text{ g m}^{-3}$ , total COD ( $120\text{--}g \text{ m}^{-3}$ ), biological oxygen demand (BOD) =  $90\text{--}200 \text{ g m}^{-3}$ , nitrate  $< 1 \text{ gN m}^{-3}$ , total nitrogen (TN) =  $20\text{--}50 \text{ gN m}^{-3}$ , sulfate =  $12\text{--}55 \text{ gS m}^{-3}$ .

**Laboratory-scale batch experiments.** Following long-term continuous-flow operation, two sets of batch experiments were performed: (i) biotransformation experiments with intact biofilm in rotating reactors (BT); and (ii) sorption experiments with re-suspended biofilm (SO). All experiments were started ( $t=0$ ) three minutes after spiking of biomarker standard solutions to ensure mixing of spiked biomarkers in solution. Figure 1 illustrates the reactor configuration and operation during BT Experiments. During the entire operation, the biofilm reactors were kept full and intermittent wetting was avoided to prevent reduction of the overall activity of the biofilm. A detailed description of each set of batch experiments is provided below. Description of all batch experiments is also presented in SI Table S2.

*Biotransformation experiments (BT).* Each rotating biofilm reactor was connected to an external container with a recirculating flow of  $4 \text{ L h}^{-1}$ . This configuration allowed for sample collection from the external container without changing the operating volume of the biofilm reactors. Two procedures were considered. The first procedure (BT-P1) was conducted by spiking a mixture containing all IS to obtain an initial ( $t=0$ ) concentration of  $10 \mu\text{g L}^{-1}$ . Following sample withdrawal during experiments, samples were immediately spiked with a mixture containing ILIS. The IS solution mixture contained the main target compounds and ILIS were used to evaluate the analytical procedure. The second procedure (BT-P2) was conducted by spiking ILIS at initial ( $t=0$ ) concentration of  $2 \mu\text{g L}^{-1}$ . In this second case only ILIS were spiked and considered the target compounds, including only MEPH-d3, METD-d3, EDDP-d3, COC-d3, BE-d3, EME-d3, CE-d3, HER-d9 and 6MAM-d3. This procedure allowed

for the improved determination of illicit drug analytes without interference of background concentrations (SI, Figure S3).<sup>13</sup>

The duration of the experiments was two days, during which 9 samples for BT-P1 and 12 samples for BT-P2 experiments were collected (around 260 mL sample volume, see SI, Figure S2). During BT-P1 experiments, additional samples were collected (i) before biomarker spiking, to measure the background concentrations; and (ii) during experiments, to monitor the biological activity of the biofilms via measurements of chemical oxygen demand (COD), sulfate (SO<sub>4</sub>-S), ammonium (NH<sub>4</sub>-N) and nitrate (NO<sub>3</sub>-N).

BT-P1 and BT-P2 experiments were conducted after continuous-flow operation of biofilm reactors for 14 and 7 months, respectively assuming biofilm reached maximum thickness. In this study, results of BT-P1 and BT-P2 experiments were used for model identification/calibration (i.e., estimation of kinetic parameters and identification of transformation pathways) and for model evaluation, respectively. For BT-P1 experiments (aerobic: pH=8.7±0.1, T=17±0.3 °C; anaerobic: pH=9.2±0.4, T=17.8±0.5 °C), and BT-P2 experiments (aerobic: pH=8.8±0.06, T=17.6±0.2 °C; anaerobic: pH=8.7±0.2, T=17.5±0.4°C), wastewater was collected from Mølleåværket WWTP (Lundtofte, Denmark). Collected pre-clarified wastewater was centrifuged (20 min, 4700 rpm) and vacuum filtered (Advantec MFS, Inc., GA-55 grade) for removal of suspended solids.

*Sorption experiments (SO).* Sorption experiments (SO) were performed with suspended aerobic biofilms (SO1) and suspended anaerobic biofilms (SO2). The experiments were conducted after 14 months of continuous-flow operation of the biofilm reactors. Tap water was circulated through the biofilm reactors for 17 h to wash-off already sorbed compounds in the biofilm. Two slides were removed from each reactor and intact biofilm was suspended in 2 L tap water for 4 h for further desorption. After centrifugation (30 min, 4700 rpm), the separated solids were mixed with 4 L vacuum filtered (Advantec MFS, Inc., GA-55 grade, pore size 6 µm) wastewater effluent (Mølleåværket WWTP, Lundtofte, Denmark). To inactivate biomass during experiment, sodium azide (0.05% v/v) was added to the mixture. The experiments were conducted for 4 h after spiking standard mixture and in total six samples (260 mL) were withdrawn. During SO1 experiment (pH=7.9±0.1, T=15.4±0.2°C) and SO2 experiment (pH=7.9±0.1, T=15.3±0.1 °C), the reactors were sparged with dried compressed air and nitrogen, respectively.

**Biofilm characterization.** The biofilm thickness (aerobic: 0.75 mm; anaerobic: 1.02 mm) was calculated by measuring biofilm volume and considering the reactor surface area of 1679 cm<sup>2</sup>. The biofilm volume was measured by filling the rotating reactors with tap water without and with biofilm inside the reactors. The difference between the volume of the empty reactor without biofilm (961 cm<sup>3</sup>) and the free volume of the reactors with biofilm (aerobic reactor, 836 cm<sup>3</sup>; anaerobic reactor, 790 cm<sup>3</sup>) was considered as the wet biofilm volume. The solids content of the biofilm was measured by re-suspending the biofilm on two removable slides into tap water, and subsequently measuring total suspended solids (TSS) and volatile suspended solid (VSS) of the mixture. The total dried mass per biofilm volume in the reactors, defined as biofilm density, was then calculated (aerobic reactor, 55 gTSS L<sup>-1</sup>, 22 gVSS<sup>-1</sup> L<sup>-1</sup>; anaerobic reactor, 83 gTSS L<sup>-1</sup>, 38 gVSS<sup>-1</sup> L<sup>-1</sup>).

**Sample preparation and chemical analyses.** Total suspended solids (TSS) were measured using gravimetric analysis after filtration (0.6 µm glass fiber filter, Advantec, USA).<sup>27</sup> Total and soluble COD, nitrate, ammonium and sulfate were measured using colorimetric methods (Hach Lange and Merck, Germany). For dissolved components, the analyses were carried out after sample filtration (0.45 µm cellulose acetate filters, Sartorius, Germany) and storage at -20 °C.

For the analysis of drug biomarkers (one sample at each sampling time), a description of sample preparation and chemical analysis by liquid chromatography coupled to high resolution mass spectrometry (HPLC-LTQ-Orbitrap) can be found elsewhere.<sup>12,28</sup> Briefly, samples were collected and immediately frozen until analysis. For samples from SO experiments samples were first filtered (0.6 µm glass fiber filter, Advantec, USA) to reduce the contact time between solids and liquid phase. Later, samples were thawed and homogenized, and 100 mL aliquots were extracted by solid phase extraction with Oasis HLB cartridges (150 mg, 6 cc, Waters, Denmark). Extracts were reconstituted in water:methanol (90:10, v/v) and 20 µL were injected into the HPLC-LTQ-Orbitrap. Separation of the target compounds was achieved in an XBridge C18 column (150 mm × 2.1 mm, I.D., particle size 3.5 µm; Waters) with a MiliQ and MeOH optimized gradient (each with 0.05% formic acid). Full scan accurate mass data were acquired in positive electrospray ionization mode over a m/z range of 50–600 Da at a resolution of 30000 full width at half maximum. For confirmation purposes, information about the fragmentation spectra of the target compounds was obtained by product-ion scan mode of the target masses



inclusion list, in the same analysis. All data were acquired and processed using Xcalibur version 2.1 software.

**Modeling framework.** The mathematical description of fate processes was formulated by accounting for temporal and spatial variation of target analyte concentrations in biofilms. Due to mass transfer limitation from the bulk phase to the biofilm and within the biofilm, concentration gradients can occur in the biofilm reactors. For the specific case of batch experiments, it was assumed that the biofilm is at steady state and as a homogeneous biomass. The volume inside the biofilm reactors was constant, whereas in the external tank the volume decreased due to withdrawal of samples. Thus, the contact time between the dissolved compounds in liquid phase and biofilm increased, which could potentially enhance biomarker transformation. Consequently, residence time dynamics were also included in the model by accounting for volume changes in the external tank (SI Figure S2). As illustrated in Figure 1, the experimental system consists of three compartments: (i) the bulk liquid in the rotating reactor, (ii) the biofilm in the rotating reactor and (iii) the external tank (continuously stirred tank reactor) connected to the biofilm reactor via a peristaltic pump. The differential equations describing mass balances in each compartment can be formulated as follows (all model parameters and state variables are listed in Table 1):

i) In the biofilm reactor bulk phase:

$$\frac{dV_R C_{R,i}}{dt} = Q_{in,R} C_{in,R,i} - Q_{out,R} C_{R,i} - j_b A_b + r_{R,i} V_R \quad (\text{eq. 1})$$

ii) In the biofilm:

$$\frac{\partial V_b C_{b,i}}{\partial t} = A_b D \frac{\partial^2 C_{b,i}}{\partial z^2} \Delta z + r_{b,i} V_b \quad (\text{eq. 2})$$

iii) In the external tank:

$$\frac{dV_T C_{T,i}}{dt} = Q_{in,T} C_{in,T,i} - Q_{out,T} C_{T,i} + r_{T,i} V_T \quad (\text{eq. 3})$$

In these formulations,  $C$  ( $\text{g m}^{-3}$ ) denotes the concentration as state variable and the subscripts  $R$ ,  $b$  and  $T$  indicate bulk phase of the rotating reactor, the biofilm, and the external tank, respectively. The volume, which is constant for the reactor bulk phase  $V_R$  ( $\text{m}^3$ ) and the biofilm  $V_b$  ( $\text{m}^3$ ), changes as a function of time inside the external tank,  $V_T$  ( $\text{m}^3$ ), as previously explained.

*Transport processes.* The flux of compounds between bulk phase and the biofilm,  $j_b$  ( $\text{g m}^{-2} \text{d}^{-1}$ ), is expressed using film theory at the mass transfer boundary layer<sup>29</sup>. The flux of compounds across the boundary layer can be defined as:

$$j_b = k_b(C_R - C_L) = \frac{D}{L_b}(C_R - C_L) \quad (\text{eq. 4})$$

Where  $k_b$  ( $\text{m d}^{-1}$ ) is the liquid-biofilm mass transfer coefficient,  $D$  ( $\text{m}^2 \text{d}^{-1}$ ) is the diffusion coefficient of the dissolved compounds into the biofilm,  $L_b$  ( $\text{m}$ ) is the biofilm thickness, and  $C_L$  is the concentration at the biofilm-liquid interface (top layer). It was assumed that no reactions occur in the boundary layer. The diffusion coefficients of target biomarkers in water,  $D_w$  ( $\text{m}^2 \text{d}^{-1}$ ) were calculated based on the revised Othmer-Thakar<sup>30</sup> equation suggested by Hayduk and Laudie<sup>31</sup>:

$$D_w = \frac{13.26 (10^{-5})}{\mu_w^{1.4} V_1^{0.589}}, \quad (\text{eq. 5})$$

where  $\mu_w$  ( $\text{kg m}^{-1} \text{s}^{-1}$ ) denotes the dynamic viscosity of water and  $V_1$  ( $\text{cm}^3 \text{g mole}^{-1}$ ) is the molar volume of the substance. Diffusion coefficients ( $D_w$ ) calculated using eq. 5 are reported in Table S1. Diffusion coefficients inside the biofilm were assumed to be reduced as compared to bulk water phase. Reduced effective diffusivity results from limitation due to increased path length in biofilm pores as compared to free aqueous media. Consequently, a dimensionless effective diffusivity factor,  $f$ , was considered:

$$D = f D_w \quad (\text{eq. 6})$$

The value of  $f$  was approximated by considering the density of the biofilm as VSS ( $\text{gVSS L}^{-1}$ ), based on the regression presented by Guimerà et al.<sup>32</sup> The boundary layer thickness,  $L_b$ , was estimated using dimensionless numbers,<sup>33,34</sup> namely Sherwood number ( $Sh$ ), Schmidt number ( $Sc$ ), Taylor number ( $Ta$ ) and Reynolds number ( $Re$ ), (see SI, eqs. S1 to S4).

*Reaction processes.* Reaction kinetics in the bulk phase of the biofilm reactor includes abiotic processes and biotransformation due to the presence of suspended biomass. The amount of suspended solids was the residuals of solids that remained in filtered wastewater (measured at  $t=0$ ) and amount of detached biomass assumed to be negligible. These processes were formulated according to the Activated Sludge Model for Xenobiotics (ASM-X) framework.<sup>12,16</sup> The reaction rate for transformation of compound  $i$  and its formation from compound  $j$  can be formulated as:

$$r_{R,i} = -k_{abio}C_{R,i} + k_{abio}C_{R,j}\frac{M_i}{M_j} - \frac{k_{bio}X_{SS}}{(1+K_{d,i}X_{SS})}C_{R,i} + \frac{k_{bio}X_{SS}}{(1+K_{d,j}X_{SS})}C_{R,j}\frac{M_i}{M_j}$$

(eq. 7)

Where  $k_{abio}$  (d<sup>-1</sup>) is the abiotic transformation rate,  $k_{bio}$  (L gTSS<sup>-1</sup> d<sup>-1</sup>) is the TSS-normalized biotransformation rate constant for the suspended solids,  $K_d$  (L gTSS<sup>-1</sup>) is the partitioning coefficient to suspended solids  $X_{SS}$  (g L<sup>-1</sup>), and  $M$  is the molecular weight. Equilibrium processes were assumed for sorption and desorption onto suspended solids.

Inside the biofilm, in addition to abiotic processes, transformation and formation processes resulted from the microbial activity of the attached biomass. The associated kinetic equations were expressed as:

$$r_{b,i} = -k_{abio}C_{R,i} + k_{abio}C_{R,j}\frac{M_i}{M_j} - k_{f,i}C_{b,i} + k_{f,j}C_{b,j}\frac{M_i}{M_j} \quad (\text{eq. 8})$$

$$k_{f,j} = \frac{k_{biof,j}X_{SS}}{(1+K_{df,j}X_{SS})} \quad (\text{eq. 9})$$

In this formulation, biofilm-mediated transformation (subscript  $f$ ) is expressed using pseudo-first order kinetics, where  $k_f$  and  $k_{biof}$  are in units of d<sup>-1</sup> and L gTSS<sup>-1</sup> d<sup>-1</sup>, respectively, and  $K_{df}$  (L gTSS<sup>-1</sup> d<sup>-1</sup>) is the partitioning coefficient in biofilms. Biofilm-mediated transformation can also be expressed by surface-normalized rate constants  $k'_{biof}$  (m<sup>3</sup> m<sup>-2</sup> d<sup>-1</sup>), obtained by dividing  $k_{biof}$  with  $X_{SS} \cdot A_b/V_b$ . The units of the reactions rates were adjusted to g m<sup>3</sup> d<sup>-1</sup> according to the units in eq. 1-3.

Finally, the reaction kinetics in the external tanks were assumed to be the same as in the bulk aqueous phase of the biofilm reactor, with additional processes for sorption and desorption to and from the tank wall<sup>12</sup>:

$$r_{T,i} = r_{R,i} - k_{des,w}k_{d,w}C_{T,i}\frac{A_T}{V_T} + k_{des,w}C_{Tw} \quad (\text{eq. 10})$$

Where  $C_{Tw}$  (g L<sup>-1</sup>) denotes the biomarker concentration sorbed onto reactor wall,  $K_{d,w}$  (m<sup>3</sup> m<sup>-2</sup> d<sup>-1</sup>) the partitioning coefficient to reactor wall. and  $k_{des,w}$  (d<sup>-1</sup>) is the desorption rate from the reactor wall.

**In-sewer transformation pathways.** Transformation and formation processes defined in eqs. 7–10 depend on the pathways identified for abiotic processes, transformation due to presence of suspended solids and biofilm-mediated transformations. The first two were adopted from our previous study.<sup>12</sup> Transformation pathways in biofilms were initially assumed based on reported human metabolic pathways.<sup>7,35</sup> This initial assumption was required due to the

absence of a priori evidence and was tested as part of the modelling study. Subsequently, any deviation from the initial pathways was assessed by examining the mass balance over suggested transformed compounds and observed transformation products (according to human metabolism).

**Model parameter estimation.** The values employed for  $k_{abio}$  and  $k_{bio}$  for suspended biomass in bulk phase were estimated in an another study.<sup>12</sup> Using SO1 and SO2 measurements (SI, Figure S8) the  $K_{df}$  values were estimated according to Ramin et al.<sup>12</sup> Values of  $k_f$  were estimated using the Bayesian optimization method Differential Evolution Adaptive Metropolis (DREAM<sub>(ZS)</sub>).<sup>36</sup> The normalized sum of squared error (SSE) was used as objective function:

$$SSE = \sum_{i=1}^n \sum_{j=1}^m \left( \frac{O_{i,j} - P_{i,j}}{O_{i,j,max} - O_{i,j,min}} \right)^2 \quad (\text{eq. 11})$$

Where  $n$  is the number of measurements series and  $m$  is the number of the data points in each series.  $O$  denotes measured data,  $P$  model predictions, and  $O_{i,j,max}$  and  $O_{i,j,min}$  the maximum and minimum of measurements, respectively. To adequately quantify the uncertainty associated to the  $k_f$  estimates, the uncertainty from  $k_{abio}$  and  $k_{bio}$  was propagated according to the identified transformation pathways for abiotic processes and biotransformation in presence of suspended solids.<sup>37</sup> Values of  $k_{biof}$  were eventually estimated based on eq. 9. We considered an upper boundary threshold of  $10^4 \text{ d}^{-1}$  for  $k_f$  in parameter estimation. Parameter estimates beyond this threshold were considered to result from model structure deficiencies (related to mass transfer).

**Model simulation and evaluation.** To simulate the transformation processes, eqs. 1–3 were numerically solved following a spatial discretization of the biofilm. Theoretically, increasing the discretization level (grid points) would increase the accuracy of prediction at the expense of higher computational time. For central grids (inside the biofilm), discretization was done using the central difference formula. Values at the first grid (biofilm-liquid interface) and the last grid points were computed via forward and backward difference, respectively. This discretization scheme was adopted from the biofilm simulation model developed by Vangsgaard et al.<sup>38</sup> The resulting set of ordinary differential equations was solved using the stiff ODE solver ode15s in Matlab R2014a (MathWorks, US). Model parameter uncertainty was assessed using the posterior probability distribution of estimates in Monte Carlo simulations as explained elsewhere.<sup>39</sup> Subsequently, the accuracy of the predictions was visually

evaluated comparing measurements from BT-P2 experiments, i.e. an independent dataset, with model predictions.

## Results and discussion

**Biological activity of biofilm reactors.** To monitor microbial activity in aerobic and anaerobic biofilms, soluble COD, sulfate and ammonium (Figure 2) as well as total COD and nitrate (SI, Figure S4) were monitored in the bulk phase during the BT-P1 experiments (while reactors were disconnected from continuous feeding). Soluble COD consisted of readily biodegradable organic substrates and soluble inert fractions, including MeOH present in the spiking solution. Utilization of MeOH as growth substrate was assumed to be negligible as in our previous study<sup>12</sup> we did not observe any substantial difference in suspended biomass growth and oxygen uptake response upon MeOH addition. Due to the likely higher activity of heterotrophic biomass under aerobic conditions as well as higher MeOH evaporation rate (dried air was sparged at a higher flow rate in the external tank compared to nitrogen gas), higher removal of soluble COD was observed in the aerobic reactor (88%) compared to the anaerobic one (57%) over 2 d. Due to the activity of sulfate reducing bacteria (SRB), sulfate was significantly reduced under anaerobic conditions (62% over 1 d) and remained constant during last day of experiment (Figure 2b). This may indicate that sulfate respiration by SRB species was limited by the absence of readily biodegradable substrate during the second day of experiment. Under aerobic conditions, the net formation (+33%) of sulfate was observed over 2 d, possibly due to biochemical oxidation of hydrogen sulfide (H<sub>2</sub>S) back to sulfate. In the aerobic BT-P1 reactor, ammonium removal is possibly dominated by assimilatory ammonia uptake. It is also reported that nitrifiers are usually overgrown by heterotrophic biomass in sewer biofilms (Huisman and Gujer, 2002; Jiang et al., 2009). Under anaerobic conditions, ammonium removal could be due to assimilation and stripping – latter due to the comparably high pH (9.2).

**Partitioning of drug biomarkers to biofilm.** Two solid-liquid partitioning coefficients were estimated for aerobic ( $K_{df,ae}$ ) and anaerobic biofilms ( $K_{df,an}$ ) using SO1 and SO2 experimental data, respectively (SI Figure S8). In addition, abiotic chemical transformation was assessed in mineral water spiked with the selected biomarkers – a study carried out previously.<sup>12</sup> These data were considered to disregard the contribution of abiotic transformation during sorption experiments. Estimated partitioning coefficients are reported in SI Table S4. The highest sorption capacity was found for THCOH ( $K_{df,ae}=2.81$  L gTSS<sup>-1</sup>;  $K_{df,an}=1.68$  L gTSS<sup>-1</sup>). The drop in THC concentration in the sorption experiments (72% in aerobic biofilms and 58% in anaerobic biofilm) can be interpreted as a result of chemical partitioning to external tank wall, as it was observed previously<sup>12</sup>, with the  $K_{df}$  values being negligible despite the high hydrophobicity of this chemical ( $\log K_{ow}=7.6$ ).<sup>40</sup> However, given the high hydrophobicity of THC, high sorption onto biofilm solids could not be ruled out, and further experimental confirmation may be required to verify our findings. Sorption of THCCOOH, EME and EDDP was only observed for anaerobic biofilms ( $K_{df,an}=1.06$  L gTSS<sup>-1</sup>;  $1.59$  L gTSS<sup>-1</sup>;  $K_{df,an}=0.15$  L gTSS<sup>-1</sup> respectively). Conversely, partitioning under aerobic conditions was found for MEPH ( $K_{df,ae}=0.20$  L gTSS<sup>-1</sup>). For the remaining chemicals, negligible sorption was observed, hence  $K_{df}$  values were set to zero. Notably, the anaerobic biofilm had higher thickness and density compared to the aerobic biofilm, which may explain the selective sorption of some of the drug biomarkers.

**Transformation of drug biomarkers.** Measurements from BT-P1 experiments were used to calibrate developed 1-D model and to predict temporal and spatial concentration profiles of drug biomarkers in the presence of sewer biofilms. Biotransformation due to the presence of suspended solids was accounted for by including previously estimated  $k_{bio}$  (L gTSS<sup>-1</sup> d<sup>-1</sup>)<sup>12,37</sup> (SI, Table S3). Measured TSS concentrations in the bulk were considered constant, namely, 42 mgTSS L<sup>-1</sup> and 104 mgTSS L<sup>-1</sup> (for BT-P1 aerobic and anaerobic, respectively) 92 mgTSS L<sup>-1</sup> and 80 mgTSS L<sup>-1</sup> (for BT-P2 aerobic and anaerobic, respectively). The abiotic transformation rates  $k_{abio}$  and partitioning coefficients of drug biomarkers to suspended solids,  $K_d$  (L gTSS<sup>-1</sup>), were set at values reported in SI, Table S3.<sup>12</sup> Subsequently, biofilm-mediated biotransformation rates  $k_f$  (d<sup>-1</sup>) and rate constants  $k_{biof}$  (L gTSS<sup>-1</sup> d<sup>-1</sup>) and  $k'_{biof}$  (m<sup>3</sup> m<sup>-2</sup> d<sup>-1</sup>) were estimated.

Measured and simulated concentration profiles of all targeted biomarkers, obtained through model calibration and validation, are presented in Figure 3. Experimental and simulation results describe removal and formation of selected

drug biomarkers in the bulk phase of the biofilm reactor, where samples were collected. The simulation results obtained through model calibration are presented using the median of the estimated parameters (full and dash lines) with the corresponding 95% credibility interval (shaded uncertainty band). The uncertainty boundary ranges, shown in Figure 3, were obtained through the propagation of the uncertainties from abiotic and biotic transformation rates (quantified here or previously<sup>12</sup>) to the model outputs. The transformation pathways identified in this study are presented in Figure S6–7. Parameter values estimated (reported as median  $\pm$  credibility interval) are listed in Table S5 and all posterior distributions of  $k_f$  values are given in Figure S11. Experimental and modelling results are presented and discussed in detail for each group of chemicals in the following paragraphs.

Prior to estimating values of  $k_f$ , the impact of discretization number (i.e. the number of layers in which the biofilm is discretized) on the prediction accuracy was assessed. The case of the aerobic transformation rates for MEPH,  $k_{f,ae,MEPH}$ , and HER,  $k_{f,ae,HER}$ , is discussed in detail (Figure 4, X-Z axis; Figure S5). HER and MEPH were chosen because they represent compounds with low and high removal rate, respectively. Discretization numbers, selected in the interval of 5-100 layers, were used to estimate  $k_f$  and using the highest level used to benchmark the level of error introduced by inaccurate model simulations. The difference is reported as relative percentage error, in which best-fit estimates for  $k_{f,ae,HER}$  and  $k_{f,ae,MEPH}$  were compared with their corresponding reference values, 214.1 d<sup>-1</sup> and 24.3 d<sup>-1</sup>, respectively. It was observed that the number of discretization had a different impact on the estimated  $k_f$  of these two chemicals, and that after 80 grid points the resulting error was negligible (< 1 %) and independent of the discretization number. This discretization number corresponds to  $\Delta Z=9.3$   $\mu\text{m}$  and  $\Delta Z=12.8$   $\mu\text{m}$  for aerobic and anaerobic biofilms, respectively.

*Mephedrone*. MEPH removal was more pronounced in the aerobic reactor (77% versus 47% in the anaerobic reactor). Higher partitioning to aerobic biofilms resulted in much higher biotransformation rate constants under aerobic conditions ( $k_{biof,ae,MEPH}=5.89$  L gTSS<sup>-1</sup> d<sup>-1</sup>,  $k_{biof,an,MEPH}=0.08$  L gTSS<sup>-1</sup> d<sup>-1</sup>). The comparably high sorption of MEPH in aerobic biofilms ( $K_{df,ae}=0.2$  L gTSS<sup>-1</sup>) makes this compound less bioavailable for microbial transformation. This impact is also reflected in eq. 9, in which  $k_{biof}$  is in the numerator and  $K_{df}$  is in denominator. Moreover, the higher aerobic  $k_{biof}$  obtained in this study agrees well with those reported previously<sup>12</sup> ( $k_{bio,ae,MEPH}=1.86$  L gTSS<sup>-1</sup> d<sup>-1</sup>,

$k_{bio,an,METD}=0$  L gTSS<sup>-1</sup> d<sup>-1</sup>). The model could adequately simulate BT-P2 dataset under both redox conditions, thereby validating the process model structure identified.

*Methadone*. Since formation of EDDP after rapid removal of METD, especially under aerobic conditions, was not observed (Fig. 3), these chemicals were considered to have independent pathways – similar to that obtained with suspended in-sewer solids.<sup>12</sup> Our analyses showed rather small deviation between duplicates (sample analysis), i.e.  $\leq 7.5\%$  for METD and  $\leq 4.5\%$  for EDDP.

Biotransformation of METD in sewer biofilms was found to be significantly faster under aerobic conditions ( $k_{biof,ae,METD}=2488$  L gTSS<sup>-1</sup> d<sup>-1</sup>,  $k_{biof,an,METD}=183$  L gTSS<sup>-1</sup> d<sup>-1</sup>), which agrees well with data obtained with in-sewer suspended solids.<sup>12</sup> Conversely, enhanced anaerobic transformation was observed for EDDP ( $k_{biof,ae,EDDP}=1.79$  L gTSS<sup>-1</sup> d<sup>-1</sup>,  $k_{biof,an,EDDP}=88.9$  L gTSS<sup>-1</sup> d<sup>-1</sup>). Simulation results (Fig. 3) for EDDP (both redox conditions) as well as for METD (only anaerobic conditions) indicate a systematic deviation between the predicted and measured values. This may imply that the model structure should be re-evaluated in future studies. A possible explanation could be related to cometabolic effects, i.e. primary substrate oxidation can enhance secondary substrate (i.e. drug biomarker) biotransformation.<sup>41–43</sup> Additionally, under anaerobic conditions, the sulfate remained constant after day 1 (Figure 2b). This may suggest that readily biodegradable substrates were depleted during the second day of experiment, resulting in negligible removal of EDDP and METD. Nevertheless, simulations could not well predict the BT-P2 dataset especially for METD, in which lower removal was observed as compared to BT-P1 measurements, as the process model do not account for cometabolic effects.

*Cocaine*. The transformation pathways for COC and its human metabolites were selected based on Bisceglia et al.<sup>44</sup> Although the biotransformation of COC to EME has been reported to be almost insignificant in raw wastewater and activated sludge<sup>16,45</sup>, in this study EME was considered as a transformation product (Fig. S6d) of COC in sewer biofilms. Accordingly, it has been reported that, in sewer biofilms, there should be another major transformation product from COC other than BE as it was speculated previously.<sup>13</sup> Net removal of COC, CE and EME and net formation of BE was observed over the duration of experiments, where BE formation resulted from hydrolysis of COC and CE.<sup>12,44</sup> Under aerobic conditions, the overall biotransformation rate constant of COC, i.e. COC to BE and COC to EME, was lower than under anaerobic conditions ( $k_{biof,ae,COC}=0.44$  L gTSS<sup>-1</sup> d<sup>-1</sup>,  $k_{biof,an,COC}=2.57$  L gTSS<sup>-1</sup> d<sup>-1</sup>). An even more pronounced deviation was observed for EME ( $k_{biof,ae,EME}=0.05$  L gTSS<sup>-1</sup> d<sup>-1</sup>,



$k_{biof,an,EME}=21.03 \text{ L gTSS}^{-1} \text{ d}^{-1}$ ), mainly due to the high biotransformation of EME in the bulk phase under aerobic conditions, SI Table S3. Aerobic and anaerobic percentage removal of COC only by sewer biofilms was found to be 3% and 33% larger than the removal observed in raw wastewater under corresponding redox conditions.<sup>12</sup> In contrast, Thai et al.<sup>13</sup> found 25% and 40% enhancement of COC removal in gravity sewer (aerobic/anaerobic) and rising sewer (anaerobic) conditions, respectively compared to removal with wastewater only. In our study, CE biotransformation kinetics obtained under aerobic and anaerobic biofilms were comparable ( $k_{biof,ae,CE}=0.68 \text{ L gTSS}^{-1} \text{ d}^{-1}$ ,  $k_{biof,an,CE}=0.51 \text{ L gTSS}^{-1} \text{ d}^{-1}$ ). BE is formed from COC and CE transformations and also transformed to another unknown transformation product ( $k_{biof,ae,BE}=2.00 \text{ L gTSS}^{-1} \text{ d}^{-1}$ ,  $k_{biof,an,BE}=0.95 \text{ L gTSS}^{-1} \text{ d}^{-1}$ ). Values of  $k'_{biof}$  ( $\text{m}^3 \text{ m}^{-2} \text{ d}^{-1}$ ) estimated in this study (SI, Table S4) for overall COC, BE and CE for aerobic biofilms ( $k'_{biof,ae,COC}=0.13 \text{ m}^3 \text{ m}^{-2} \text{ d}^{-1}$ ,  $k'_{biof,ae,BE}=0.57 \text{ m}^3 \text{ m}^{-2} \text{ d}^{-1}$ ,  $k'_{biof,ae,CE}=0.39 \text{ m}^3 \text{ m}^{-2} \text{ d}^{-1}$ ) are almost 4 times, 34 and 2 times higher than the values reported by McCall et al.<sup>14</sup> (aerobic biofilms at 21°C). In contrary, for BE, no transformation by in-sewer suspended solids and sewer biofilms was reported.<sup>13</sup> The differences are possibly due to different microbes residing in the biofilms in these studies.

*Heroin.* Transformation of heroin biomarkers was assumed to follow the pathways previously described for human metabolism<sup>24,35,46</sup>, namely two-step deacetylation to 6MAM and to MOR. MORG was also considered to be transformed to MOR via deconjugation.<sup>47</sup> It was hypothesized that COE was not only transformed to NCOE by sewer biofilms but also to MOR as it was observed in raw wastewater under anaerobic conditions.<sup>37</sup> Nevertheless, biofilm-mediated biotransformation processes could be described with transformation pathways similar to human metabolism. HER was rapidly removed in both sewer biofilms (similarly to raw wastewater (SI, Figure S9), with higher biotransformation kinetics in anaerobic biofilms ( $k_{biof,ae,HER}=4.43 \text{ L gTSS}^{-1} \text{ d}^{-1}$ ,  $k_{biof,an,HER}=22.14 \text{ L gTSS}^{-1} \text{ d}^{-1}$ ). Likewise, a five-fold increase of 6MAM biotransformation kinetics was observed in anaerobic biofilms ( $k_{biof,ae,6MAM}=1.11 \text{ L gTSS}^{-1} \text{ d}^{-1}$ ,  $k_{biof,an,6MAM}=6.45 \text{ L gTSS}^{-1} \text{ d}^{-1}$ ). These differences cannot be explained only by considering differences in the removal of 6MAM in aerobic and anaerobic biofilms (i.e. 33% and 59% in aerobic and anaerobic biofilms in 12 h experimental time (SI, Figure S9). Thus, additional processes are assumed to be involved, notably, the formation of 6MAM from HER. Given that the 6MAM biotransformation by in-sewer suspended solids is significantly lower than in biofilms, the total % removal is not substantially different from those

reported by Thai et al.<sup>13</sup> However, McCall et al.<sup>14</sup> found 3 times higher biotransformation rate for 6MAM by aerobic biofilm compared to in-sewer suspended solids. In this study, as to pathway identification, no additional transformation product of HER was considered when assessing the conservation of HER mass. Moreover, MORG was found to be transformed only by anaerobic sewer biofilm ( $k_{biof,an,MORG}=2.03 \text{ L gTSS}^{-1} \text{ d}^{-1}$ ) – a rate approximately 6 times lower than that by in-sewer suspended biomass.<sup>12</sup> Due to rapid aerobic transformation of MORG in the bulk, no aerobic biofilm-induced removal was observed for MORG. High transformation of MORG was also observed by Senta et al.<sup>8</sup> in wastewater.

Biotransformation rates obtained for COE and NOE in biofilms are at a moderate level, with NCOE having higher transformation under anaerobic conditions. The simulation model identified can effectively simulate the fate of HER and 6-MAM transformation in the BT-P2 independent datasets, thereby validating the modelling approach.

*THC*. In untreated wastewater, THCOH was not found to be a transformation product of THC.<sup>12</sup> Accordingly separate transformation pathways were assumed for THC and THCOH in sewer biofilms. Based on pathways suggested in literature,<sup>35</sup> THCCOOH was considered to be formed from THCOH.<sup>35</sup> As a result of poor data quality, no clear conclusion could be drawn for THC biotransformation especially under anaerobic conditions. Moreover, the  $k_{biof,ae,THC}=0$  as THC removal was completely attributed to partitioning to the external tank and abiotic hydrolysis. Hence, model calibration could not be performed using THC data set (SI, Figure S10). THCOH exhibited comparably high biotransformation rate constants ( $k_{biof,ae,THCOH}=21034 \text{ L gTSS}^{-1} \text{ d}^{-1}$ ,  $k_{biof,an,THCOH}=5066 \text{ L gTSS}^{-1} \text{ d}^{-1}$ ), which were also observed for THCCOOH biotransformation in the anaerobic biofilm ( $k_{biof,an,THCCOOH}=3272 \text{ L gTSS}^{-1} \text{ d}^{-1}$ ).

We note that the high  $k_{biof}$  values corresponded to high  $K_{df}$  values for these chemicals (SI Table S4), a factor that makes THCOH and THCCOOH less bioavailable for biotransformation. Interestingly, aerobic THCCOOH biotransformation obtained ( $k_{biof,ae,THCCOOH}=133 \text{ L gTSS}^{-1} \text{ d}^{-1}$ ) was lower than that under anaerobic conditions.

**The impact of mass transfer limitation.** Compared to common growth substrates, illicit drug biomarkers are relatively large molecules. The average molar volume,  $V_l$  ( $\text{cm}^3 \text{ mol}^{-1}$ ), of biomarkers in this study is  $250 \text{ cm}^3 \text{ mol}^{-1}$ , significantly larger than the molar volume of readily biodegradable substrates

such as acetate ( $56.1 \text{ cm}^3$ ).<sup>48</sup> Therefore, the comparably high molar volume is assumed to significantly impact diffusivity of drug biomarkers in biofilm.

In general, the concentration in the boundary layer is proportional to the ratio of convective mass transfer (i.e. axial flow in biofilm reactor) to diffusive mass transport ( $Sh$  number). According to eq. 5, molecules with a higher molar volume and low diffusivity are expected to have lower boundary layers (SI Figure S1). In biofilm modeling studies, typically an average boundary layer is assumed for all chemicals, under the condition that this approximation does not impact the accuracy of predictions; this, however, is generally done without proper error assessment. Figure 4 (Y-Z axis) illustrates the impact of the choice of boundary layer thickness on the accuracy of estimation of biotransformation rate,  $k_f$ , for the example of MEPH and HER in aerobic biofilms. Estimated values for a range of boundary layer thicknesses (5 to 100  $\mu\text{m}$ ) together with discretization number (10 to 100) were compared with reference predictions for MEPH (30  $\mu\text{m}$ ) and HER (20  $\mu\text{m}$ ) with discretization number of 100. These results indicate that the impact of the boundary layer thickness on parameter estimates (i) is compound-specific; and (ii) varies by the discretization number employed (Figure 4 X-Z axis). A higher influence was observed for more reactive compounds, i.e. HER, at lower discretization numbers. In Figure 4, red dots denote the values employed in this study (discretization number=80 layers; boundary layer thickness=23  $\mu\text{m}$ ). Furthermore, diffusion of HER and MEPH was compared in aerobic and anaerobic biofilms through simulation of diffusive transport, considering negligible partitioning to solids and transformation (SI Figure S12). Following the spiking of internal standards in BT-P1 experiments, the concentrations in the bulk phase of the reactors were predicted to reach an equilibrium level after 2 h in aerobic biofilms and 4 h in anaerobic biofilms. These delays show the impact of mass transfer limitation across the boundaries of biofilm and liquid phase – a factor that necessitates an effective diffusion modelling for which we provided an example here. Moreover, the recirculation between external tank and reactor cause additional limiting step for reaching equilibrium. An example of concentration profile inside the biofilm is also presented for MEPH (SI, Figure S13).

#### **Transformation in raw wastewater and sewer biofilms – A comparison.**

Biotransformation rate constants in sewer biofilms  $k_{biof}$  estimated in this study were compared rate constants in the presence of suspended solids,  $k_{bio}$  (Figure 5).<sup>12</sup> Under aerobic conditions (reproducing a gravity sewer), most biomarkers exhibited similar  $k_{biof}$  and  $k_{bio}$  values (see error bars in Figure 5). Biofilm-mediated transformations were found to be dominant for COE and NCOE, whilst

the majority of MORG and MOR transformation occurred in the bulk water by suspended biomass. Under anaerobic conditions, MEPH, METD, COC, EME, CE, THCOH, and THCCOOH were found to be biotransformed only in biofilms. Moreover, no additional major transformation products for HER and MORG, other than 6MAM and MOR, respectively, were identified in the biofilm reactors, as opposed to raw wastewater.

**Future perspectives.** In this study, we assessed the transformation of 16 drug biomarkers in biofilm reactors under aerobic and anaerobic conditions, representing typical conditions in gravity and pressure sewers (respectively). This investigation complemented our previous study<sup>12</sup> on the fate of drug biomarkers in raw sewage, in the presence of suspended biomass only. A comparative assessment of the results indicates that sewer biofilms enhance the transformation kinetics of many of selected drug biomarkers, particularly under anaerobic conditions (Figure 5), likely due to higher anaerobic activity in biofilms than in suspended biomass. Under aerobic conditions, transformation kinetics in biofilms was overall comparable to that observed for untreated sewage, indicating again limited stability of selected biomarkers. This evidence suggests the necessity of accounting for biofilm-mediated transformation when predicting in-sewer fate of drug biomarkers. Moreover, for the reliable prediction of trace organic chemical fate in biofilm, the mathematical consistency of simulation model structures should be assessed.

More observations are needed to validate sorption and transformation of THC in sewer biofilms. In this study all drug biomarkers (parents and metabolites) were spiked simultaneously to simulate environmentally-relevant conditions, i.e. the occurrence of drug biomarkers in sewer as a mixture. The developed model however could describe the transformations among biomarkers. Nevertheless, future experimental designs used could benefit from spiking unrelated biomarkers (e.g., in separate batch experiments) or using biomarkers with several different labels, although resulting in a drastic increase of the cost of chemical analysis.

The microbial activity of the two biofilms in this study was characterized by monitoring utilization of primary substrates (e.g., organic carbon, sulfate) during batch experiments. Our results showed substantial differences in microbial activity between the two biofilms assessed in this study, e.g., significantly higher sulfate-reducing activity in the anaerobic biofilm. In sewer systems, microbial functions and community of sewer biofilms vary over a sewer length likely as a result of changes in boundary conditions and gradients in substrate

concentrations and wastewater composition. To date, this has been demonstrated for gravity sewers<sup>14</sup>. Hence, further research is required to characterize microbial activity of the sewer biofilms at different sewer locations and correlate the microbial community and activity with biotransformation rates.

In this study, the aeration was performed in a separate tank and not directly in the biofilm reactor. The objective was to provide sufficient oxygen supply to ensure that most microorganisms would be exposed to aerobic conditions. It should be noted that (re)aeration may be different in full-scale sewer systems, being caused by flow fluctuations and mixing. The current study potentially offers the background for a combined modelling framework for real sewers, where switching functions based on dissolved oxygen concentration would allow differentiating between aerobic and anaerobic conditions.

Although this study compared the biotransformation rate in raw wastewater and in biofilms, the contribution of each of these biotransformation processes to the overall drug biomarkers removal should be assessed. Moreover, the assessment of drug abuse rates at catchment level should account for, importantly, the layout of the sewer system, hydraulic conditions<sup>49</sup> and the possible drug release patterns. Additionally, model-based back-calculation tools should account for abiotic processes and biotransformation induced by suspended biomass and sewer biofilms.<sup>50</sup> Hence, a reactive-transport model needs to be developed, describing drug biomarkers transformation under steady-state and dynamic conditions. Transformation rates estimated in this study can be used to calibrate such simulation models. Our ongoing research<sup>50</sup> is addressing the impact of neglecting in-sewer biotransformation on estimation of daily drug consumption in catchments using uncertainty analysis and measurements from sampling campaigns. Results presented in this study underscore the high level of complexity of in-sewer biomarker fate, of which the implications to wastewater-based epidemiological engineering are numerous.

## Acknowledgments

This study was supported by the European Union's Seventh Framework Programme for research, technological development and demonstration [grant agreement 317205, the SEWPROF MC ITN project]. Borja Valverde-Pérez thanks the Technical University of Denmark (DTU) for the financial support through the KAIST-DTU project on Integrated Water Technology (InWaTech, <http://www.inwatech.org>).

## Reference

- (1) Thomas, K. V.; Bijlsma, L.; Castiglioni, S.; Covaci, A.; Emke, E.; Grabic, R.; Hernández, F.; Karolak, S.; Kasprzyk-Hordern, B.; Lindberg, R. H.; et al. Comparing illicit drug use in 19 European cities through sewage analysis. *Sci. Total Environ.* **2012**, *432*, 432–439.
- (2) Daughton CG. Illicit drugs in municipal sewage: proposed new non-intrusive tool to heighten public awareness of societal use of illicit/abused drugs and their potential for ecological consequences. In *American Chemical Society, Symposium Series*; American Chemical Society, Symposium Series: Washington, DC, 2001; p 348–364.
- (3) Hvitved-Jacobsen, T.; Vollertsen, J.; Matos, J. S. The sewer as a bioreactor - A dry weather approach. *Water Sci. Technol.* **2002**, *45* (3), 11–24.
- (4) Jelic, A.; Rodriguez-Mozaz, S.; Barceló, D.; Gutierrez, O. Impact of in-sewer transformation on 43 pharmaceuticals in a pressurized sewer under anaerobic conditions. *Water Res.* **2014**, *68*, 98–108.
- (5) McCall, A.-K.; Bade, R.; Kinyua, J.; Lai, F. Y.; Thai, P. K.; Covaci, A.; Bijlsma, L.; van Nuijs, A. L. N.; Ort, C. Critical review on the stability of illicit drugs in sewers and wastewater samples. *Water Res.* **2016**, *88*, 933–947.
- (6) Castiglioni, S.; Bijlsma, L.; Covaci, A.; Emke, E.; Hernández, F.; Reid, M.; Ort, C.; Thomas, K. V.; Van Nuijs, A. L. N.; De Voogt, P.; et al. Evaluation of uncertainties associated with the determination of community drug use through the measurement of sewage drug biomarkers. *Environ. Sci. Technol.* **2013**, *47* (3), 1452–1460.
- (7) van Nuijs, A. L. N.; Abdellati, K.; Bervoets, L.; Blust, R.; Jorens, P. G.; Neels, H.; Covaci, A. The stability of illicit drugs and metabolites in wastewater, an important issue for sewage epidemiology? *J. Hazard. Mater.* **2012**, *239–240*, 19–23.
- (8) Senta, I.; Krizman, I.; Ahel, M.; Terzic, S. Assessment of stability of drug biomarkers in municipal wastewater as a factor influencing the estimation of drug consumption using sewage epidemiology. *Sci. Total Environ.* **2014**, *487*, 659–665.
- (9) Baker, D. R.; Očenášková, V.; Kvicálová, M.; Kasprzyk-Hordern, B. Drugs of abuse in wastewater and suspended particulate matter - Further developments in sewage epidemiology. *Environ. Int.* **2012**, *48*, 28–38.
- (10) Baker, D. R.; Kasprzyk-Hordern, B. Critical evaluation of methodology commonly used in sample collection, storage and preparation for the analysis of pharmaceuticals and illicit drugs in surface water and wastewater by solid phase extraction and liquid chromatography-mass spectrometry. *J. Chromatogr. A* **2011**, *1218* (44), 8036–8059.
- (11) Polesel, F.; Andersen, H. R.; Trapp, S.; Plósz, B. G. Removal of Antibiotics in Biological Wastewater Treatment Systems □ A Critical Assessment Using the Activated Sludge Modeling Framework for Xenobiotics (ASM-X). *Environ. Sci. Technol.* **2016**, *50* (19), 10316–10334.
- (12) Ramin, P.; Brock, A. L.; Polesel, F.; Causanilles, A.; Emke, E.; de Voogt, P.; Plósz, B. G. Transformation and sorption of illicit drug biomarkers in sewer systems: understanding the role of suspended solids in raw wastewater. *Environ. Sci. Technol.* **2016**, *50* (24), 13397–13408.
- (13) Thai, P. K.; Jiang, G.; Gernjak, W.; Yuan, Z.; Lai, F. Y.; Mueller, J. F. Effects of

- sewer conditions on the degradation of selected illicit drug residues in wastewater. *Water Res.* **2014**, *48*, 538–547.
- (14) McCall, A.-K.; Scheidegger, A.; Madry, M. M.; Steuer, A. E.; Weissbrodt, D. G.; Vanrolleghem, P. A.; Kraemer, T.; Morgenroth, E.; Ort, C. Influence of different sewer biofilms on transformation rates of drugs. *Environ. Sci. Technol.* **2016**, *50* (24), 13351–13360.
- (15) Ort, C.; Gujer, W. Sorption and high dynamics of micropollutants in sewers. *Water Sci. Technol.* **2008**, *57* (11), 1791–1797.
- (16) Plósz, B. G.; Reid, M. J.; Borup, M.; Langford, K. H.; Thomas, K. V. Biotransformation kinetics and sorption of cocaine and its metabolites and the factors influencing their estimation in wastewater. *Water Res.* **2013**, *47* (7), 2129–2140.
- (17) Bisceglia, K. J.; Lippa, K. a. Stability of cocaine and its metabolites in municipal wastewater - the case for using metabolite consolidation to monitor cocaine utilization. *Environ. Sci. Pollut. Res.* **2014**, *21* (516), 4453–4460.
- (18) Jiang, F.; Leung, D. H.-W. W.; Li, S.; Chen, G.-H. H.; Okabe, S.; van Loosdrecht, M. C. M. A biofilm model for prediction of pollutant transformation in sewers. *Water Res.* **2009**, *43* (13), 3187–3198.
- (19) Schwarzenbach, R. P.; Gschwend, P. M.; Imboden, D. M. *Environmental Organic Chemistry*; Wiley Interscience: Hoboken, NJ, 2003.
- (20) Wicke, D.; Böckelmann, U.; Reemtsma, T. Experimental and modeling approach to study sorption of dissolved hydrophobic organic contaminants to microbial biofilms. *Water Res.* **2007**, *41* (10), 2202–2210.
- (21) Torresi, E.; Polesel, F.; Bester, K.; Christensson, M.; Smets, B. F.; Trapp, S.; Andersen, H. R.; Plósz, B. G. Diffusion and sorption of organic micropollutants in biofilms with varying thicknesses. *Water Res.* **2017**.
- (22) Huisman, J. L.; Gujer, W. Modelling wastewater transformation in sewers based on ASM3. *Water Sci. Technol.* **2002**, *45* (6), 51–60.
- (23) EMCDDA. *European Drug Report*; 2017.
- (24) Boerner, U.; Abbott, S.; Roe, R. L. The Metabolism of Morphine and Heroin in Man. *Drug Metab. Rev.* **1975**, *4* (1), 39–73.
- (25) Rochex, A.; Godon, J.; Bernet, N.; Escudie, R. Role of shear stress on composition , diversity and dynamics of biofilm bacterial communities. *Water Res.* **2008**, *42*, 4915–4922.
- (26) Oms, C.; Gromaire, M. C.; Saad, M.; Milisic, V.; Chebbo, G.; Gromaire, M. C.; Saad, M.; Milisic, V.; Bed, G. C. Bed shear stress evaluation in combined sewers. *Urban Water J.* **2008**, *5* (3), 219–229.
- (27) APHA. *Standard methods for the examination of water and wastewater. American Public Health Association*, 19th ed.; Washington, D.C, 1995.
- (28) Bijlsma, L.; Emke, E.; Hernández, F.; de Voogt, P. Performance of the linear ion trap Orbitrap mass analyzer for qualitative and quantitative analysis of drugs of abuse and relevant metabolites in sewage water. *Anal. Chim. Acta* **2013**, *768* (1), 102–110.
- (29) Horn, H.; Hempel, D. C. Modeling mass transfer and substrate utilization in the

- 792 boundary layer of biofilm systems. *Water Sci. Technol.* **1998**, 37 (4–5), 139–147.
- 793 (30) Othmer, D. F.; Thakar, M. S. Correlating Diffusion Coefficients in Liquids. *Ind. Eng.*  
794 *Chem.* **1953**, 45 (3), 589–593.
- 795 (31) Hayduk, W.; Laudie, H. Prediction of diffusion coefficients for nonelectrolytes in  
796 dilute aqueous solutions. *AIChE J.* **1974**, 20 (3), 611–615.
- 797 (32) Guimerà, X.; Dorado, A. D.; Bonsfills, A.; Gabriel, G.; Gabriel, D.; Gamisans, X.  
798 Dynamic characterization of external and internal mass transport in heterotrophic  
799 biofilms from microsensors measurements. *Water Res.* **2016**, 102, 551–560.
- 800 (33) Wanner, O.; Eberl, H. J.; Morgenroth, E.; Noguera, D. R.; Picoreanu, C.; Rittmann,  
801 B. E.; van Loosdrecht, M. C. . *Mathematical modeling of biofilms*; 2006.
- 802 (34) Recktenwald, A.; Lücke, M.; Müller, H. W. Taylor vortex formation in axial through-  
803 flow: Linear and weakly nonlinear analysis. *Phys. Rev. E* **1993**, 48 (6), 4444–4454.
- 804 (35) Castiglioni, S.; Zuccato, E.; Fanelli, R. *Illicit Drugs in the Environment: Occurrence,*  
805 *Analysis, and Fate Using Mass Spectrometry*; JohnWiley & Sons, Inc, 2011.
- 806 (36) Laloy, E.; Vrugt, J. a. High-dimensional posterior exploration of hydrologic models  
807 using multiple-try DREAM(ZS) and high-performance computing. *Water Resour.*  
808 *Res.* **2012**, 48 (1), 1–18.
- 809 (37) Ramin, P.; Valverde-Pérez, B.; Polesel, F.; Locatelli, L.; Plósz, B. G. A systematic  
810 model identification method for chemical transformation pathways – the case of  
811 heroin biomarkers in wastewater. *Sci. Report, Accept. with Revis.* **2017**.
- 812 (38) Vangsgaard, A. K.; Mauricio-Iglesias, M.; Gernaey, K. V.; Smets, B. F.; Sin, G.  
813 Sensitivity analysis of autotrophic N removal by a granule based bioreactor: Influence  
814 of mass transfer versus microbial kinetics. *Bioresour. Technol.* **2012**, 123, 230–241.
- 815 (39) Sin, G.; Gernaey, K. V.; Neumann, M. B.; van Loosdrecht, M. C. M.; Gujer, W.  
816 Uncertainty analysis in WWTP model applications: A critical discussion using an  
817 example from design. *Water Res.* **2009**, 43 (11), 2894–2906.
- 818 (40) Rosa Boleda, M.; Huerta-Fontela, M.; Ventura, F.; Galceran, M. T. Evaluation of the  
819 presence of drugs of abuse in tap waters. *Chemosphere* **2011**, 84 (11), 1601–1607.
- 820 (41) Plósz, B. G.; Langford, K. H.; Thomas, K. V. An activated sludge modeling  
821 framework for xenobiotic trace chemicals (ASM-X): Assessment of diclofenac and  
822 carbamazepine. *Biotechnol. Bioeng.* **2012**, 109 (11), 2757–2769.
- 823 (42) Torresi, E.; Fowler, J. S.; Polesel, F.; Bester, K.; Andersen, H. R.; Smets, B. F.; Plósz,  
824 B. G.; Christensson, M. Biofilm thickness influences biodiversity in nitrifying  
825 MBBRs – Implications on micropollutant removal. *Environ. Sci. Technol.* **2016**, 50  
826 (17), 9279–9288.
- 827 (43) Sathyamoorthy, S.; Chandran, K.; Ramsburg, C. A. Biodegradation and Cometabolic  
828 Modeling of Selected Beta Blockers during Ammonia Oxidation. *Environ. Sci.*  
829 *Technol.* **2013**, 47, 12835–12843.
- 830 (44) Bisceglia, K. J.; Roberts, A. L.; Lippa, K. A. A hydrolysis procedure for the analysis  
831 of total cocaine residues in wastewater. *Anal. Bioanal. Chem.* **2012**, 402, 1277–1287.
- 832 (45) Bisceglia, K. J. K.; Lippa, K. a. Stability of cocaine and its metabolites in municipal  
833 wastewater - the case for using metabolite consolidation to monitor cocaine



834 utilization. *Environ. Sci. Pollut. Res.* **2014**, *21* (6), 4453–4460.

835 (46) Stefanidou, M.; Athanasis, S.; Spiliopoulou, C.; Dona, A.; Maravelias, C.  
836 Biomarkers of opiate use. *Int. J. Clin. Pract.* **2010**, *64* (12), 1712–1718.

837 (47) Castiglioni, S.; Zuccato, E.; Crisci, E.; Chiabrando, C.; Fanelli, R.; Bagnati, R.  
838 Identification and measurement of illicit drugs and their metabolites in urban  
839 wastewater by liquid chromatography-tandem mass spectrometry. *Anal. Chem.* **2006**,  
840 *78* (24), 8421–8429.

841 (48) ACD/I-Lab 2.0 Prediction Software by Advanced Chemistry Development Inc.  
842 (ACD/Labs).

843 (49) McCall, A.; Palmitessa, R.; Blumensaat, F.; Morgenroth, E.; Ort, C. Modeling in-  
844 sewer transformations at catchment scale – Implications on drug consumption  
845 estimates in wastewater-based epidemiology. *Water Res.* **2017**.

846 (50) Ramin, P. Modelling Illicit Drug Fate in Sewers for Wastewater-Based  
847 Epidemiology, PhD Thesis, Technical University of Denmark, 2016.

848

849

850 **Table 1.** Model state variables and parameters

Symbol	Definition	Units	Values
$A_b$	Biofilm area	$\text{m}^2$	$4 \cdot 10^{-3}$
$C_R$	Concentration of drug biomarkers in reactor	$\text{g L}^{-1}$	
$C_b$	Concentration of drug biomarkers inside biofilm	$\text{g L}^{-1}$	
$C_T$	Concentration of drug biomarkers in external tank bulk phase	$\text{g L}^{-1}$	
$C_{Tw}$	Concentration of drug biomarkers sorbed onto external tank wall	$\text{g L}^{-1}$	
$d$	Gap between rotating drum and stationary cylinder ( $R_2 - R_1$ )	m	0.012
$d_R$	Reactor Characteristic length ( $2d$ )		0.024
$D$	Diffusion coefficient of the soluble compounds into the biofilm	$\text{m}^2 \text{d}^{-1}$	Table S2
$D_w$	Diffusion coefficient of the soluble compounds in water	$\text{m}^2 \text{d}^{-1}$	Table S2
$f$	Dimensionless effective diffusivity	-	ae:0.68 an:0.38
$j_b$	Flux of compounds between bulk phase and the biofilm	$\text{g m}^{-2} \text{d}^{-1}$	
$k_b$	Mass transfer coefficient between bulk phase and the biofilm	$\text{m d}^{-1}$	
$k_{des,w}$	Desorption from reactor wall	$\text{d}^{-1}$	100
$K_{dw}$	Reactor wall–liquid partition coefficient	$\text{m}^3 \text{m}^{-2}$	Ramin et al. <sup>12</sup>
$K_d$	Suspended Solid–liquid partition coefficient	$\text{L gTSS}^{-1}$	Ramin et al. <sup>12</sup>
$K_{df}$	Suspended biofilm–liquid partition coefficient	$\text{L gTSS}^{-1}$	Table S4
$k_{abio}$	Abiotic transformation rate constant	$\text{d}^{-1}$	Ramin et al. <sup>12</sup>
$k_{bio}$	TSS-normalized biotransformation rate constant	$\text{L gTSS}^{-1} \text{d}^{-1}$	Ramin et al. <sup>12</sup>
$k_f$	Sewer biofilm biotransformation rate (eq. 9)	$\text{d}^{-1}$	Figure S11
$k_{biof}$	TSS-normalized Sewer biofilm biotransformation rate	$\text{L gTSS}^{-1} \text{d}^{-1}$	Table S4
$k'_{biof}$	Area-to-volume-normalized Sewer biofilm biotransformation rate	$\text{m}^3 \text{m}^{-2} \text{d}^{-1}$	Table S4
$L_b$	Concentration boundary layer	m	$23 \cdot 10^{-6}$
$M$	Biomarker molecular weight	$\text{g mol}^{-1}$	Table S2
$O$	Observed (measured) values		
$P$	Predicted (simulated) values		
$Q_{in,R}$	Reactor inflow	$\text{m}^3 \text{d}^{-1}$	$4 \cdot 10^{-3}$
$Q_{out,R}$	Reactor outflow	$\text{m}^3 \text{d}^{-1}$	$4 \cdot 10^{-3}$
$Q_{in,T}$	External tank inflow	$\text{m}^3 \text{d}^{-1}$	$4 \cdot 10^{-3}$
$Q_{out,T}$	External tank outflow	$\text{m}^3 \text{d}^{-1}$	$4 \cdot 10^{-3}$
$r_R$	Reaction rate in reactor	$\text{g L d}^{-1}$	
$r_b$	Reaction rate in side biofilm	$\text{g L d}^{-1}$	
$r_T$	Reaction rate in external tank	$\text{g L d}^{-1}$	
$R_1$	Reactor inner radius (outer radius of rotating drum)	m	0.045
$R_2$	Reactor outer radius (inner radius of stationary cylinder)	m	0.057
$V_R$	Total reactor volume	$\text{m}^3$	$9.61 \cdot 10^{-4}$
$\bar{u}$	Average axial velocity inside reactor (a continuous operation; b: batch experiment)	$\text{m s}^{-1}$	a: $0.12 \cdot 10^{-4}$ a: $2.89 \cdot 10^{-4}$
$V_b$	Biofilm volume	$\text{m}^3$	ae: $1.25 \cdot 10^{-4}$ an: $1.71 \cdot 10^{-4}$
$V_T$	Bulk volume in external volume	$\text{m}^3$	Figure S2
$V_I$	Molar volume	$\text{cm}^3 \text{g mole}^{-1}$	Table S2
$X_{SS}$	Concentration of suspended solids	$\text{gTSS L}^{-1}$	Table S3
$\Delta Z$	Discretization distance inside biofilm for spatial discretization of partial differential equations	m	ae: $9.3 \cdot 10^{-6}$ an: $12.8 \cdot 10^{-6}$
$\mu_w$	Dynamic viscosity of water (at $\sim 17^\circ \text{C}$ )	$\text{kg m}^{-1} \text{s}^{-1}$	$1.07 \cdot 10^{-3}$
$\nu$	Kinematic viscosity of water (at $\sim 17^\circ \text{C}$ )	$\text{m}^2 \text{s}^{-1}$	$1.07 \cdot 10^{-6}$
$\sigma_w$	Wet-surface-to-volume ratio	$\text{m}^2 \text{m}^{-3}$	Figure S2
$\Omega$	Angular velocity of rotating drum	$\text{rad d}^{-1}$	2.09

851

852

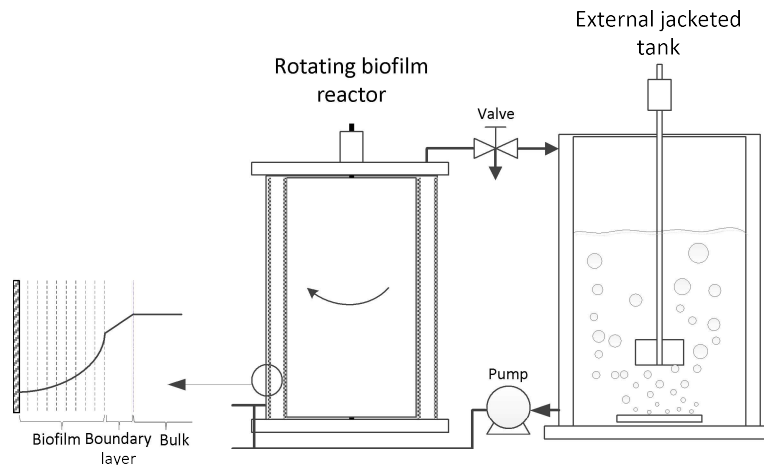


**Figure 1.** Configuration of rotating biofilm reactor (on the left) connected to an external tank (on the right) during batch experiments. The samples were taken from the outlet of the biofilm reactor, on the top valve. Anaerobic or aerobic conditions were maintained in the external tank by sparging air or nitrogen, respectively, from a diffuser placed at the bottom of the tank. A typical drug concentration profile inside the biofilm is also presented.

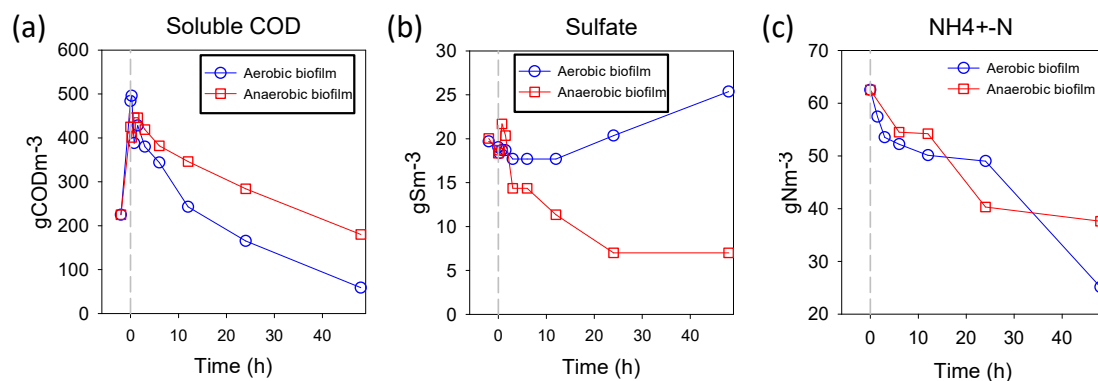


**Figure 2.** Soluble COD, sulfate and ammonium concentrations measured during BT-P1 experiments under aerobic and anaerobic conditions. Measurements before  $t=0$  refer to samples taken prior to the spiking of standards, and the subsequent increase of soluble COD concentration at  $t=0$  should be associated with the addition of MeOH resulting from spiking of biomarkers mixture. Lines connecting data points are based on simple linear interpolation to show the trends.

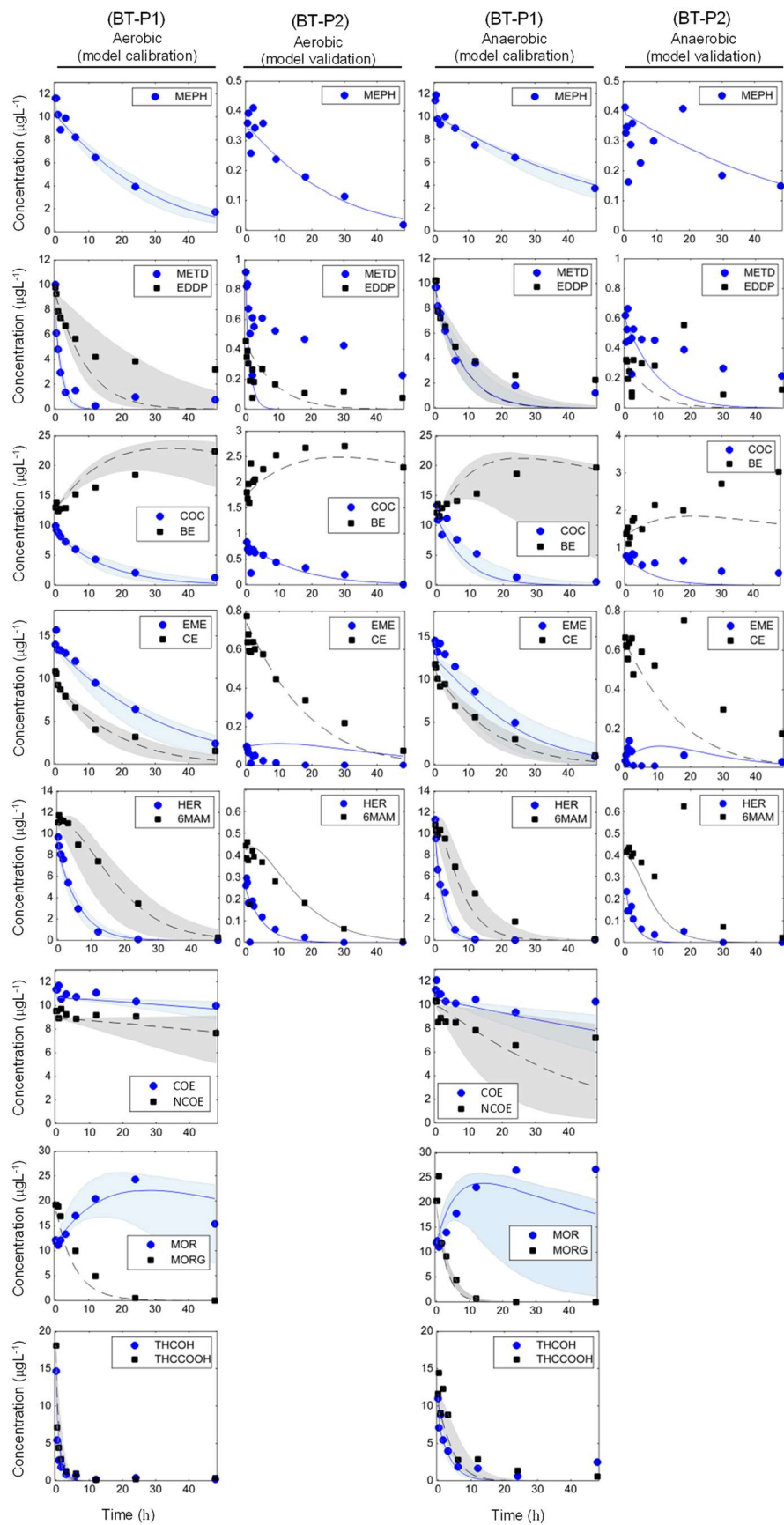


**Figure 3.** Experimental data and simulation results for biomarker transformations in sewer biofilm under aerobic and anaerobic conditions. Results are related to model calibration using BT-P1 experimental data and model validation using BT-P2 experimental data. THC data is presented in (SI, Figure S10). Markers are measured data and lines are simulation results. The shaded areas reflect 95% credibility interval of model prediction.

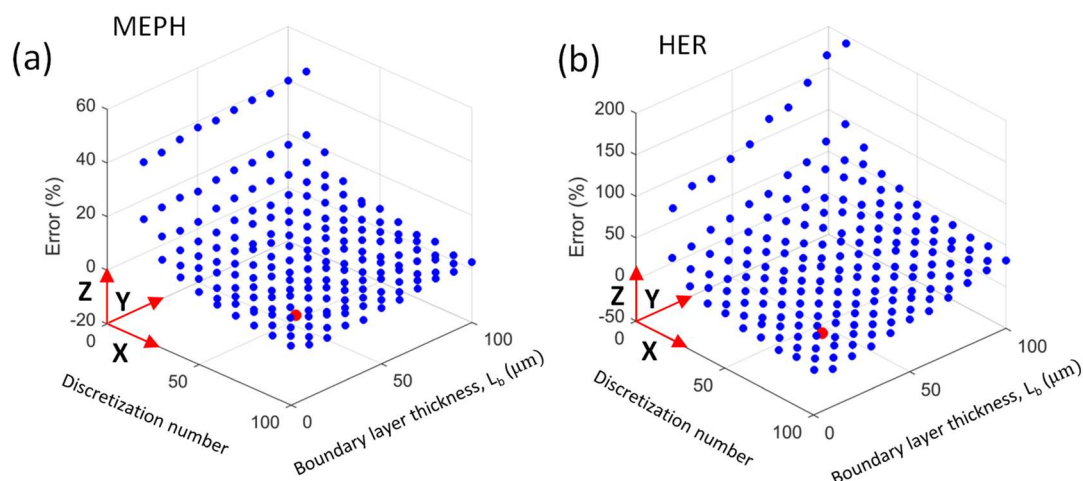


**Figure 4.** The impact of discretization number (number of discretization layers considered for numerical integration in biofilm) and boundary layer thickness on estimation of aerobic transformation rate,  $k_f$  ( $d^{-1}$ ), for MEPH and HER. 190 scenarios were considered for each chemical. The parameter estimate at each scenario was compared with the reference scenario for each chemical. The reference scenario contained 100 layers using the accurate estimation of boundary layer thickness, i.e. 30  $\mu m$  for MEPH and 20  $\mu m$  for HER. Blue dots are the data resulted from scenarios and red dots correspond to the values chosen in this study (i.e. 80 discretization number and 23  $\mu m$  boundary layer thickness). Considering this choice resulted in an acceptable error i.e. 0.4% for MEPH and 2% for HER.

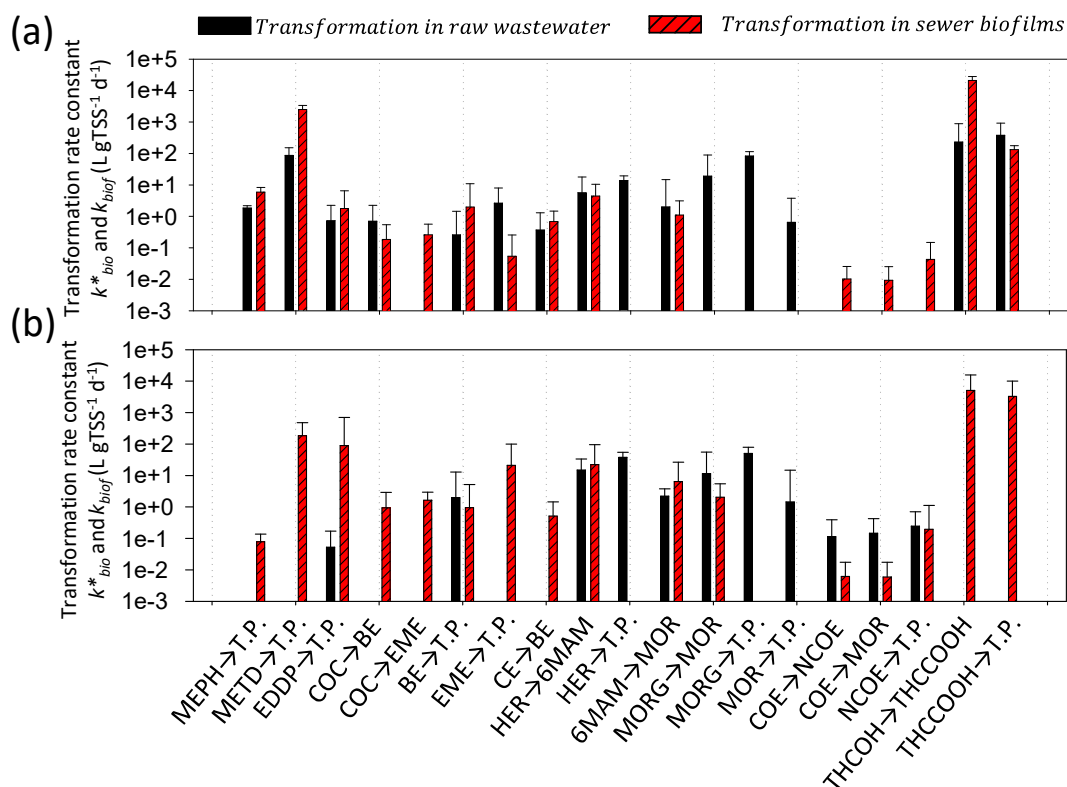


**Figure 5.** Comparing the biotransformation of drug biomarkers in raw wastewater and bio-transformation in sewer biofilms under aerobic (a), and anaerobic (b) conditions. For this comparison, TSS-normalized transformation rate constants in raw wastewater  $k_{bio}$  ( $L\ gTSS^{-1}\ d^{-1}$ ) reported in Ramin et al.<sup>12</sup> are compared with sewer biofilm-mediated transformation rate constants,  $k_{biof}$  ( $L\ gTSS^{-1}\ d^{-1}$ ), from this study. Error bars identify the upper bound of the 95% credibility interval of estimated parameters.

